Sorption and Transport Studies of Water in Kapton* Polymide. I

D. K. YANG, W. J. KOROS,† H. B. HOPFENBERG, and V. T. STANNETT, *Department of Chemical Engineering, North Carolina State University, Raleigh, North Carolina 27650*

Synopsis

Sorption isotherms and diffusion coefficients of water in a 0.3-mil Kapton polyimide film at 30, 45, and 60°C are reported. The data are well described by the dual mode sorption and transport models at low activities. At high penetrant activities, clustering of water is suggested by a Zimm–Lundberg analysis of the sorption data and the fact that the diffusion coefficient for water decreases with increasing external vapor activity. The effect of temperature on the diffusion coefficients at infinite dilution and the dual mode sorption parameters k_D, b, and C_H' are presented and discussed. The magnitude of the activation energy of the diffusion coefficient at infinite dilution, 5.4 kcal/mol, is smaller than the corresponding activation energy in more flexible chain polymers, perhaps suggesting that rather small backbone motions are associated with diffusion of water through the Kapton matrix. The predictions for the isosteric enthalpy of sorption from the dual mode model are presented and compared with the values determined from graphical analysis of the sorption isotherms performed independently without reference to the dual mode sorption model.

INTRODUCTION

Surprising changes in polymer physical properties can occur as a result of the presence of relatively small quantities of sorbed water, especially for hydrogen bonding polymers. For example, the modulus of nylon increases with water content over the temperature range from 155 to 250 K,[1–5] under which conditions water appears to hydrogen-bond with the amide groups of the nylon backbone and functions as mechanically stable bridges between chains in the amorphous region.[1,2,6,7] At higher temperatures the thermally driven agitation of the water molecules and the chain segments tend to disrupt the hydrogen bonding. At higher water activities, the presence of sorbed water can lower the effective glass transition temperature of the sample and dramatic changes in modulus may occur.[1–5] The loss compliance of the material,[8] impact strength, ductility, toughness, and the dielectric constant associated with the α-relaxation[1,2,9] are increased with water content.

Kapton, which is the subject of the present paper, is a commercially important aromatic polyether diimide with the structure shown below. Kapton, like nylon shows antiplasticization at all temperatures below about 300 K in the presence of water due to hydrogen bond formation[10–16] and

* Registered trademark, E. I. du Pont de Nemours and Company.

† The Center for Energy Studies, The University of Texas at Austin, Austin, TX 78712.

Journal of Applied Polymer Science, Vol. 30, 1035–1047 (1985)
 CCC 0021-8995/85/031035-13$04.00

hole filling. At room temperature and above, the modulus is almost independent of water content[11,15,16].

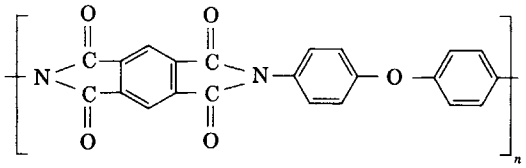

Kapton polyimide

Kapton's excellent thermal stability and good mechanical and insulation properties[10] make it an important material in the aerospace and microelectronic industries. Whereas previous investigators have focused on characterization of the water vapor permeability of Kapton,[17-19] it was our objective to make direct gravimetric measurements of water sorption uptake and kinetics to corroborate the previous indirect values of water vapor solubility estimated from steady state permeation and transient time lag measurements.

Due to the nature of the glassy state, nonequilibrium chain conformations exist and give rise to unrelaxed gaps between segments on neighboring polymer chains. This excess volume results in the presence of additional environments into which a penetrant can sorb compared to the situation pertaining to a truly densified equilibrium glass. During sorption, penetrants sorb into both the densified polymer matrix and the preexisting microvoids. This physical phenomenon is referred to as "dual mode sorption" and is modeled as a superposition of a Henry's law or Flory–Huggins dissolution term and a Langmuir term associated with saturation of the preexisting microvoid volume.

A rather unusual form for the concentration dependent diffusion coefficient involving a maximum at an intermediate concentration was observed in our study of water interactions with polyacrylonitrile.[20] It was of interest to determine if a similar effect was observed with Kapton since the maximum, while unusual, was easily explained in terms of combined dual mode sorption effects at low concentrations and clustering and/or plasticizing at higher sorbed concentrations.

EXPERIMENTAL

Materials

The 0.3 mil (7.62×10^{-6} m) thick Kapton polyimide films used in this study were uncoated amorphous samples which were kindly provided by the E. I. du Pont de Nemours and Company. The density of the film is reported to be 1.42 g/cc.[10] DSC studies using a Perkin–Elmer Differential Scanning Calorimeter II failed to show a measurable glass transition[21,22] because the change of C_p was not significant due to the subtle increase in motion of the Kapton chain at T_g. However, T_g is reported to be in the temperature range 350–450°C, which is confirmed by Wrasidlo[23] by means of dynamic mechanical and dielectric methods. High purity distilled, deion-

ized water was subjected to three freeze/thaw cycles under vacuum to remove any traces of dissolved gases prior to use in sorption experiments.

Equipment and Procedures

The design and operation of the McBain quartz spring balance used in this study have been described previously by our group.[20,21,24,25] With this system, a direct gravimetric measure of penetrant uptake by the polymer as a function of time can be determined by observing changes in spring extension. In the cell the polymer sample was hung at the base of the spring, and a glass reference fiber was hung parallel to the spring to compensate for small shifts in the spring support position. The sorption cell was maintained at a constant temperature by circulating fluid such as deionized H_2O from a bath through a fluid jacket surrounding a cell.

The integral sorption–desorption method was used in this study. The system, excluding the sorption cell, was pressurized with penetrant to an empirically determined value that would give the desired sorption pressure when the stopcock to the sorption cell was opened. At time zero, the penetrant was admitted into the sorption cell, and the spring extension was measured as a function of time. To begin a desorption experiment, the valve connecting the sorption cell to the vacuum line was opened, and the contraction of the spring was observed as a function of time.

RESULTS AND DISCUSSION

Sorption

Sorption isotherms for water in the 0.3-mil Kapton film at 30°C, 45°C, and 60°C are shown in Figure 1. Based on these isotherms, small but dis-

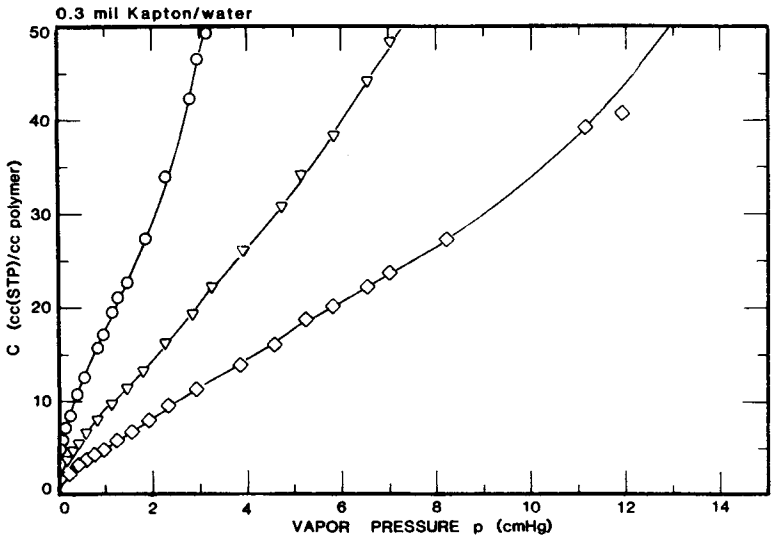

Fig. 1. Sorption isotherms for water in Kapton of 0.3 mil thickness at 30°C (○), 45°C (▽), and 60°C (◇) plotted vs. vapor pressure.

cernable dual mode sorption effects are apparent as concavity of the isotherm with respect to the pressure axis at low vapor pressure. The most common interpretation given to isotherms which display such concavity is that there is a finite amount of unrelaxed volume which can be saturated as the vapor activity increases.[26] An alternative physical interpretation might be to suppose that the apparent site saturation process which gives rise to the concavity is due to a strong hydrogen bonding. Mathematically, the two treatments are rather similar since both envision a saturation mechanism. The saturation capacity can be evaluated using the simple dual mode sorption formalism as described immediately below.

At higher vapor activities, the sorption isotherms display curvature convex to the pressure axis. These effects will be discussed later in the context of the Zimm–Lundberg clustering analysis.

Dual Mode Sorption at Low Activities. At low vapor activities, the sorption isotherms shown in Figure 1 are concave to the pressure axis and can be described analytically by the dual-mode sorption model given by

$$C = k_D p + \frac{C'_H b p}{1 + bp} \tag{1}$$

where C [cc(STP)/cc polymer] is the equilibrium concentration of water in the polymer at a pressure p, k_D [(cc(STP)/cc polymer · cm Hg)] is the Henry's law solubility coefficient, b [(cm Hg)$^{-1}$] is the affinity constant of the gas or vapor for the Langmuir sites, and C'_H [cc(STP)/cc polymer)] is the maximum capacity of the polymer for the penetrant in the unrelaxed gaps presumed to comprise the Langmuir environment in the polymer.

The dual mode coefficients k_D, C'_H, and b, shown in Table I, were estimated using SAS nonlinear regression analysis program,[27] based on the low activity sorption data in Figure 1. The Henry's law constant k_D characterizes the sorption of penetrant in a polymer by a mechanism which involves separation of the polymer chains to accommodate the penetrant molecule. A van 't Hoff expression describes the temperature dependence of k_D:

$$k_D = k_{D0} \exp(-\Delta H_D / RT) \tag{2}$$

where ΔH_D is the enthalpy difference between the penetrant in the Henry's law sorbed state and in the vapor. A similar van 't Hoff relationship may be written for b, the affinity constant of penetrant for the Langmuir sorption sites:

$$b = b_0 \exp(-\Delta H_b / RT) \tag{3}$$

TABLE I
Dual Mode Sorption Parameters k_D,C'_H, and b at Different Temperatures

T (°C)	k_D [cc(STP)/cc polymer · cm Hg]	C'_H [cc(STP)/cc polymer]	b (cm Hg)$^{-1}$]
30	11.209	6.553	26.466
45	5.744	3.389	13.715
60	3.071	2.304	8.757

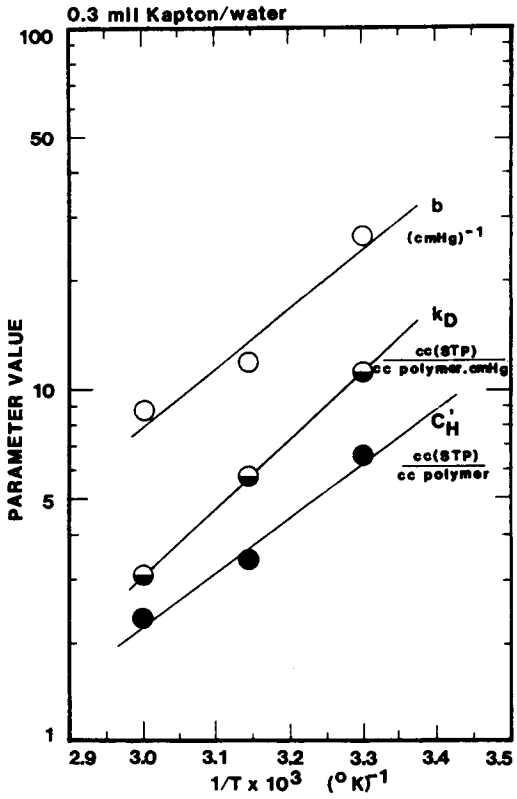

Fig. 2. Van 't Hoff plot of k_D (=) [cc (STP)/(cc) polymer · cm Hg)], b (=) (cm Hg)$^{-1}$ and C'_H (=) (cc(STP)/cc polymer) for H_2O sorption in Kapton film of 0.3 mil thickness.

where ΔH_b is the difference between the enthalpy of the penetrant in the Langmuir sorbed state and that in the vapor phase.

Normally, one might anticipate that sorption into preexisting gaps would be more exothermic than the corresponding case in which energy must be supplied to prepare a place for the penetrant. The van 't Hoff plot in Figure 2, however, gives $\Delta H_D = -8.718$ kcal/g · mol and $\Delta H_b = -7.43$ kcal/g · mol. While this difference is rather small, we believe it is significant. Previous measurements[21] of SO_2 sorption in Kapton indicated that ΔH_D exceeded ΔH_b by 2.1 kcal/g · mol, again, a rather surprising result. The presence of a residual solvent[21] in Kapton has been verified, and it has been shown previously that a residual solvent can produce the somewhat anomalous effects related to the relative magnitude of ΔH_D and ΔH_b.[28,29] In the case of H_2O sorption in polyacrylonitrile, the enthalpy of sorption, ΔH_b, changed from -10.1 to -11.7 kcal/g·mol following a rigorous solvent exchange protocol to remove the trace solvent from this polymer.[30,31]

The experimentally determined Langmuir capacities for both Kapton/SO_2 and Kapton/H_2O systems as a function of temperature are presented in Figure 3. The Langmuir capacities, based on the prediction by Koros and Paul,[32] should decrease with temperature and disappear around T_g. Two straight lines, as Figure 3 illustrates, approximate satisfactorily the two sets of experimental results over the range of experimental temperature. The extrapolation of the two straight lines to the temperature abscissa,

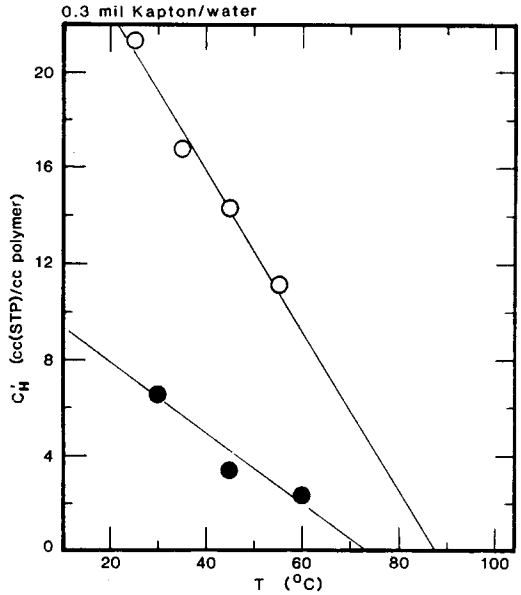

Fig. 3. Langmuir capacities for SO_2 (○) and H_2O (●) in Kapton polyimide as a function of experimental temperature.

however, yield the intercepts 73°C and 88°C for Kapton/H_2O and Kapton/SO_2 systems, respectively, while the T_g of Kapton, reported by Wrasidlo,[23] is between 350°C and 450°C. Several papers[12,13,15,16,23] indicate the presence of a β-transition temperature of Kapton in the temperature range 80–120°C. Possibly, the decline of C'_H is also related to small transitions such as β, γ, δ, $\cdots$ in glassy polymer in addition to the α-transition temperature.[21] This effect may cause a gradual elimination of frozen unrelaxed volume with C'_H at the β- and α-transitions. Due to experimental equipment constraints, it was not possible to perform measurements above the β-transition temperature to verify this suggestion.

Cluster Formation at High Activities. The upturn in the sorption isotherms presented in Figure 1 at high vapor activities, coupled with evidence to be discussed later that the effective local diffusion coefficient decreases with increasing concentration at high activities, suggests that penetrant clustering is occurring under these conditions. The so-called "clustering function", G_{11}/v_1, as shown in eq. (4), was developed by Zimm and Lundberg[33,34] based on the statistical mechanics of fluctuations. This function was used to estimate the cluster size for a binary component system:

$$\frac{G_{11}}{v_1} = -\phi_2 \left[\frac{\partial(a_1/\phi_1)}{\partial a_1} \right]^1_{P,T} \tag{4}$$

where the subscript 1 refers to the penetrant, v_1 is the partial molar volume of the penetrant, G_{11} is the clustering integral, ϕ_1 is the volume fraction of penetrant in the polymer film, a_1 is the activity of the penetrant, and a_1/ϕ_1 is the volume fraction activity coefficient.

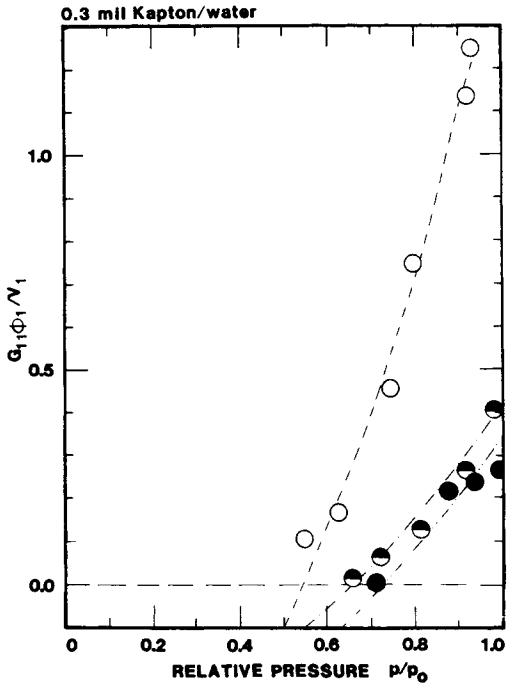

Fig. 4. The average number of penetrant molecules in the neighborhood of a given penetrant molecule in excess of the mean concentration of penetrant in the polymer $G_{11}\phi_1/v_1$ plotted vs. relative pressure in 0.3 mil Kapton at 30°C (●), 45°C (◓), and 60°C (○).

The composite parameter $\phi_1 G_{11}/v_1$ is equal to the average number of penetrant molecules in the neighborhood of a given penetrant molecule in excess of the mean concentration.[33] The activity dependence of a_1/ϕ_1 and G_{11}/v_1 can be obtained by numerical differentiation of a polynomial fit of the sorption data or by graphical differentiation of the sorption data. For $G_{11}/v_1 > -1$ clustering of the penetrant is likely. Zimm–Lundberg clustering parameters, calculated from the data by numerical differentiation of fourth order polynomial fit to the data in Figure 1, are presented in Figure 4. The data indicate that clustering is measurable ($\phi_1 G_{11}/v_1 > 0$) for activities above 0.50–0.65 depending on the temperature studied.

The cluster formation of H_2O in rubbery polymers is generally exothermic owing to the ease of moving polymer chains above T_g and the strong negative energies of interaction possible between two or more clustered water molecules.[35] On the other hand, the net heat effect for clustering in the glassy polymer can be endothermic. This fact may be rationalized in terms of the extra energy required to separate the stiff chains to accommodate penetrant clusters. These arguments, of course, are consistent with the observation that the cluster formation tends to be initiated at lower activities at higher temperatures in Kapton and other glasses.[30,35,36]

Isosteric Sorption Enthalpy. The isosteric sorption enthalpy[37] ΔH_I is a measure of the average difference in enthalpy between a molecule in the sorbed state and in the gaseous state measured at constant penetrant sorbed concentration. The isosteric sorption enthalpy is given by

$$\frac{\Delta H_I}{R} = -z\left[\frac{d \ln p}{d(1/T)}\right]_C \tag{5}$$

where z is the compressibility factor, R is the gas constant, and p (cm Hg) is the water vapor pressure corresponding to concentration C at the temperature T selected for isosteric evaluation. The resultant experimental values of ΔH_I, determined from the slope of plots of ln p vs. $1/T$ at 45°C using $z = 1$, are plotted as the points in Figure 5 as a function of concentration C.

The temperature dependence of the Langmuir capacity, C'_H, is believed to be due to variation in the unrelaxed volume in the glass rather than due to a true energetic effect, e.g., polymer–penetrant interaction. However, there is still considerable discussion concerning the nature of the temperature dependence of the sorption isotherms and the temperature dependence of C'_H can be described phenomenologically be a van 't Hoff type expression such as eq. (2). The apparent sorption enthalpy ΔH^* obtained from the slope of the van 't Hoff plot in Figure 2 is -7.0 kcal/g · mol. The variation of ΔH_I with concentration can be predicted using the following equation for systems that obey dual-mode sorption theory[37]:

$$\Delta H_I = z\left(\frac{k_D\Delta H_D + C'_H\Delta H_T E - C'_H\Delta H_b pE^2}{k_D + C'_H E - C'_H pE^2}\right) \tag{6}$$

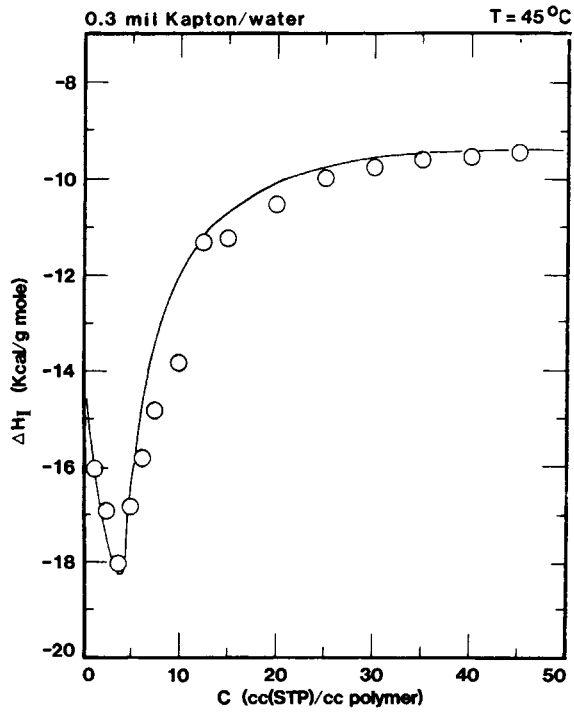

Fig. 5. Isosteric enthalpies of sorption for H_2O in 0.3 mil Kapton film plotted vs. sorbed water concentration: (—) predicted value; (⊙) experimental data.

where $\Delta H_T = \Delta H_b + \Delta H^*$ and $E = b/(1 + bp)$

The solid line in Figure 5 was calculated using eq. (6) with dual mode parameters and p corresponding to C at 45°C. The agreement with experimental points is good for concentrations below 7.5 cc(STP)/cc polymer with a slight deviation between the calculated line and the experimental data at higher concentrations. Interestingly, the asymptotic value of the isosteric enthalpy is extremely close to that of the enthalpy of condensation of water vapor at 45°C ($\Delta H_C = -10.3$ kcal/g · mol). This suggests a rather small heat of mixing at high concentration.

Diffusion Coefficient. Diffusion coefficients D of water vapor in Kapton film were calculated using the long-time approximate solution to the infinite series solution for sorption–desorption kinetic data at different activities. For large fractional uptakes, i.e., $\frac{M_t}{M_\infty} > 0.6$,[38] the long-time approximate sorption kinetic result is given by

$$M_t/M_\infty = 1 - 8/\pi^2 \exp(-D\pi^2 t/l^2) \tag{7}$$

where M_t and M_∞ are the mass sorbed (or desorbed) at time t and at "infinite" time, respectively, and l is the film thickness. Plots of $\ln[1 - M_t/M_\infty]$ vs. t yielded the slope $D\pi^2/l^2$. D values calculated in this way correspond to the average concentration dependent diffusion coefficient defined by

$$\overline{D} = (D_s + D_d)/2 \tag{8}$$

where D_s and D_d are diffusion coefficients obtained from the slope of the above plots for sorption and desorption respectively. The average coefficient $\overline{D}$, defined in Figure 6, may be approximated by eq. (9) over the concentration interval $C_{\text{initial}} - C_{\text{final}}$, chosen for study:

$$\overline{D} \simeq \frac{\int_{C_{initial}}^{C_{final}} D_{\text{eff}}(C)\, dC}{C_{\text{final}} - C_{\text{initial}}} \tag{9}$$

The variation of diffusion coefficients with concentration calculated from eq. (8) at three different temperatures is presented in Figure 6. The lines in Figure 6 represent a fourth-order polynomial fit of the $D(C)$ vs. C data and the circles represent the average experimental value for a large number of runs in each interval of activity. At 60°C, the sorption equilibrium were reached much more quickly than that at lower temperatures, particularly at low activities; therefore, less accuracy of the data at 60°C could be achieved. The range of variability of diffusion coefficient for each activity interval is given in the Table II. The cause of larger variability of the diffusion coefficients in the lower activities at 60°C was never achieved. The average values of diffusion coefficient shown in Figure 6 are the results of a large number of sorption kinetic runs for the activity range of 0–0.1 and 0.1–0.2. These average values appear to be consistent with the trend of low

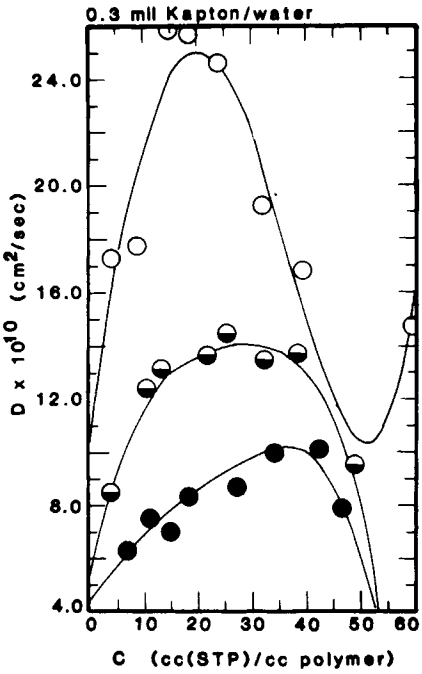

Fig. 6. Concentration dependent diffusion coefficient $D(C)$ estimated from long time approximation based on sorption kinetics data at 30°C (●), 45°C (◒), and 60°C (○). The lines represent the fourth-order approximation fit and the circles represent the experimental data.

temperature runs presumably; therefore, the scattering observed at low activities for 60°C was simply due to difficulty in precisely measuring short sorption half-time and small mass uptake for this condition.

For vapor activities above 0.5 only one point was measured due to much greater precision of the measurements in the higher activity ranges where sorption levels were more substantial. The data at all temperatures appear to show a well-defined trend of $D(C)$ vs. C, which can be described reasonably well by the fourth-order polynomial form shown as the lines in Figure 6. The three lines indicate that D increases at low concentration and then decreases with concentration after D reaches the maximum. Similar behavior has been observed for water diffusion in polyacrylonitrile (PAN).[20] The increase of diffusion coefficient with concentration can be explained in terms of the dual mode sorption model.[26] The decrease of diffusion coefficient at high concentrations is consistent with the occurrence of clustering suggested by the isotherm shapes reported in Figure 1.

TABLE II
Maximum Range of Variability of the Diffusion Coefficient as a Function of Activity at 60°C

$a = p/p_0$	C [cc(STP)/cc polymer]	$\bar{D}$ (cm²/s)
0–0.1	0–9.4	5.04×10^{-10}–3.21×10^{-9}
0.1–0.2	9.4–13.3	9.25×10^{-10}–2.31×10^{-9}
0.2–0.3	13.3–17.0	1.62×10^{-9} –3.45×10^{-9}
0.3–0.4	17.0–20.5	1.42×10^{-9} –3.87×10^{-9}
0.4–0.5	20.5–25.1	2.26×10^{-9} –2.65×10^{-9}

The maximum point in the $D(C)$ vs. C curves in Figure 6 shifts to lower activities as the temperature increases, suggesting that clustering begins at lower activities at high temperature, again consistent with the Zimm–Lundberg analysis. Similar behavior in the PAN/H_2O system was observed.[39] An Arrhenius plot of the infinite dilution diffusion coefficient D^0 is presented in Figure 7. The effective activation energy for diffusion of water in Kapton at infinite dilution is found from the slope of this plot to be only +5.43 kcal/g·mol. The rather small value of this activation energy suggests that the compact water molecule requires the localization of extremely small packets of volume in the vicinity of a given penetrant to permit the execution of a diffusion jump. On the contrary, the considerably larger SO_2, CO_2, and O_2 molecule exhibited activation energies of 10.55, 8.6, and 7.4 kcal/g·mol, respectively.[21,40,41] This result is qualitatively consistant with one's expectations since the size of the transient gap that must open next to a given penetrant is larger for large molecules than for small ones like H_2O.

CONCLUSION

As in the polyacrylonitrile (PAN)/H_2O system, the sorption isotherm and concentration dependent diffusion coefficient of water in Kapton can be well described by the dual mode sorption model at low concentrations. At higher sorbed concentrations clustering of water molecules appears to occur, based on both sorption and diffusion behavior. The maximum point of the $D(C)$ vs. C curve, corresponding to the onset of clustering, is shifted to lower concentrations with increasing temperature. This suggests that the formation of water clusters in Kapton is an endothermic process. The analysis of the temperature dependence of dual mode parameters k_D and b shows the same type of abnormal difference between ΔH_D and ΔH_b as was observed in as-received PAN films. These PAN films were found to contain small

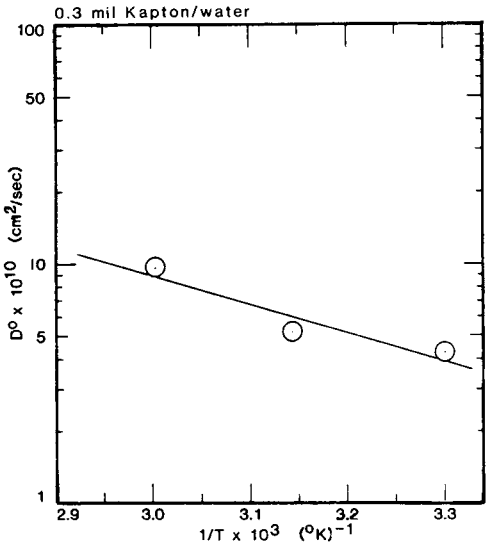

Fig. 7. Arrhenius plot of D^0 at infinite dilution in 0.3 mil Kapton/H_2O system.

amounts of a low molecular weight residual. Evidence of a small amount of low molecular weight residual has been noted by previous authors working with Kapton. The sorption enthalpy result is not surprising when viewed in the context of the dual mode sorption model. This model, in fact, predicts such behavior under certain conditions for low volatility residual solvents.

The authors gratefully acknowledge the support of this work by the grant of the Army Research Office Grant DAAG 29-81-K-0039. We appreciate the assistance of Dr. An Wang in glassblowing and Mrs. Mary Wade and Miss Christy Beltz in typing.

References

1. P. E. Bretz, R. W. Hertzberg, J. A. Manson, and A. Ramirez, in *Water in Polymer*, S. P. Rowland, Ed., Am. Chem. Soc., Washington, D.C., 1980, Chap. 32, p. 531.
2. H. W. Starkweather, Jr., in *Water in Polymer*, S. P. Rowland, Ed. by Am. Chem. Soc., Washington, D.C., 1980, Chap. 25, p. 433.
3. H. W. Starkweather, Jr., *J. Macromol. Sci.*, **B3**(4), 727 (1969).
4. J. M. R. Quistwater and B. A. Dunell, *J. Polym. Sci.*, **28**, 309–318 (1958).
5. A. E. Woodward, J. M. Crissman, and J. A. Sauer, *J. Polym. Sci.*, **44**, 23 (1960).
6. R. Puffr and J. Sebenda, *J. Polym. Sci. C*, **16**, 79–93 (1967).
7. N. G. McCrum, B. F. Read, and G. Williams, *Anelastic and Dielectric Effects in Polymeric Solids*, Wiley, New York, 1967.
8. M. T. Hahn, R. W. Hertzberg, J. A. Manson, R. W. Lang, and P. E. Bretz, *Polymer*, **23**, 2675 (1982).
9. H. W. Starkweather, Jr. in *Nylon Plastics*, M. V. Kohan, Ed., Wiley, New York, 1973.
10. "Kapton Polyimide Film-Summary of Properties," E. I. DuPont Company, Wilmington, Del., 1981.
11. J. A. Sauer and T. Lim, *Polym. Repr.*, **17**(2), 43 (1976).
12. G. A. Bernier and D. E. Kline, *J. Appl. Polym. Sci.*, **12**, 593 (1968).
13. G. E. Butta, S. de Petris, and M. Pasquini, *J. Appl. Polym. Sci.*, **13**, 1073 (1969).
14. R. M. Ikeda, *Polym. Lett.*, **4**, 353 (1966).
15. T. Lim, V. Frosini, V. Zaleckas, D. Morrow, and J. A. Sauer, *Polym. Eng. Sci.*, **13**, 51 (1973).
16. T. Lim, PhD. dissertation, Rutgers University 1967.
17. W. H. Hubbell, Jr., H. Brandt, and Z. A. Munir, *J. Polym. Sci., Polym. Phys. Ed.*, **13**, 493 (1975).
18. E. Sacher and J. R. Susko, *J. Appl. Polym. Sci.*, **23**, 2355 (1979).
19. E. Sacher and J. R. Susko, *J. Appl. Polym. Sci.*, **26**, 679 (1981).
20. V. T. Stannett, G. R. Ranade, and W. J. Koros, *J. Membr. Sci.*, **10**, 219–233 (1982).
21. R. M. Felder, C. J. Patton, and W. J. Koros, *J. Polym. Sci., Polym. Phys. Ed.*, **19**, 1995 (1981).
22. C. J. Patton, MS thesis, North Carolina State University, Raleigh, 1980.
23. W. Wrasidlo, *J. Macromol. Sci. Phys.*, **B6**(3), 559 (1972).
24. C. H. M. Jacques and H. B. Hopfenberg, *Polym. Eng. Sci.*, **14**, 441 (1974).
25. L. R. Iler, R. C. Laundon, and W. J. Koros, *J. Appl. Polym. Sci.*, **27**, 1163–1175 (1982).
26. R. T. Chern, W. J. Koros, E. S. Sander, S. H. Chen, and H. B. Hopfenberg, *Implications of the Dual-Mode Sorption and Transport Models for Mixed Gas Permeation*, ACS Symposium Series, No. 223 Am. Chem. Soc., Washington, D.C., 1983, p. 47.
27. *SAS User's Guide*, J. T. Helwig and K. A. Concil, Eds., SAS Instituter Statistical Analysis System, Cary, N.C., 1979.
28. W. J. Koros, G. N. Smith, and V. T. Stannett, *J. Appl. Polym. Sci.*, **26**, 159–170 (1981).
29. W. J. Koros, *J. Polym. Sci., Polym. Phys. Ed.*, **18**, 981 (1980).
30. G. Ranade, V. Stannett, and W. J. Koros, *J. Appl. Polym. Sci.*, **25**, 2179–2186 (1980).
31. M. Haider, PhD dissertation, North Carolina State University, Raleigh, 1978.
32. W. J. Koros and D. R. Paul, *J. Polym. Sci., Polym. Phys. Ed.*, **16**, 1947 (1978).
33. B. H. Zimm and J. L. Lundberg, *J. Phys. Chem.*, **60**, 425 (1956).
34. J. L. Lundberg, *J. Macromol. Sci. Phys.*, **B3**(4), 693–710 (1969).
35. J. A. Barrie and D. Machin, *Trans. Faraday Soc.*, **67**, 244 (1971).

36. G. R. Ranade, PhD dissertation, North Carolina State University, Raleigh, 1979.
37. W. J. Koros, D. R. Paul, and G. S. Huvard, *Polymer,* **20**, 956 (1979).
38. J. Crank and G. S. Park, in *Diffusion in Polymer,* J. Crank and G. S. Park, Eds., Academic, New York, 1968.
39. V. Stannett, M. Haider, W. J. Koros, and H. B. Hopfenberg, *Polym. Eng. Sci.,* **20**, 300 (1980).
40. W. J. Koros, J. Wang, and R. M. Felder, *J. Appl. Polym. Sci.,* **26**, 2805 (1981).
41. R. T. Chern, PhD dissertation, North Carolina State University, Raleigh, 1983.

Received November 10, 1983
Accepted July 12, 1984